



Laser Multi-mode Scanning Thermography Method for Fast Inspection of Micro-cracks in TBCs Surface

Dacheng Jiao¹ · Wenxiong Shi^{1,2} · Zhanwei Liu¹ · Huimin Xie²

Received: 12 September 2017 / Accepted: 30 March 2018 / Published online: 6 April 2018
© Springer Science+Business Media, LLC, part of Springer Nature 2018

Abstract

Conventional non-destructive testing methods are difficult to be applied in defect detection of thermal barrier coating (TBCs) because of some of its characteristics, such as porosity and thin thickness, etc. For detecting surface cracks in TBCs, a laser multi-modes scanning thermography (SMLT) method has been developed in this paper, combining fast scan mode using linear laser with fine scan mode using point laser on the tested specimen surface. Linear scanning has a large detection range and detection speed, and point scanning has a higher sensitivity. Through the theoretical analysis, numerical simulation and experimental verification, five unique thermal response features of the cracks stimulated by two scanning modes were discovered and summarized. These features in the thermal images include temperature sharply rising in local region, distinct increase of the area of high temperature zone, obvious ‘tailing’, ‘dislocation’ and thermal obstruction phenomenon, respectively. Therefore, with the corresponding post-processing algorithm developed here, the location and shape of surface cracks in TBCs can be efficiently detected by analyzing the information of these thermal response features. Validation tests showed that the surface cracks with the width of more than 20 μm can be quickly detected in line-scan stage, while in point-scan stage, the 9.5 μm wide surface cracks can be accurately detected.

Keywords Laser multi-mode scanning thermography · Thermal barrier coatings · Surface crack · Threshold segmentation

1 Introduction

Thermal barrier coatings (TBCs) have been widely used in a variety of gas turbine and diesel engine [1]. TBCs structure, usually consisting of substrate, bond coat and ceramic coat, is a typical multilayer system and each layer has markedly different physical, thermal and mechanical properties. The premature failure mechanism of TBCs has not yet been clearly understood by now because of its complex structure and extremely harsh service environment. Surface cracks in ceramic coating and interface cracks along the thermally grown oxide interface (TGO) are the two main failure modes in TBCs [2,3]. It is worth noting that a deep surface crack

with a certain width may form a passage for high temperature and oxygen, which accelerates the generation and extension of interface crack and eventually makes TBCs off from the substrate in advance [4,5].

At any rate, nondestructive testing of surface crack in TBCs is apparently important and indispensable for both the application and the improvement of the coating structure. Due to intrinsic properties of TBCs, such as porosity, ultra-thin thickness (100–400 μm), and nonconductive, etc., some traditional NDT methods such as ultrasonic test, eddy current testing and impedance detection, have limitations with regard to the detection efficiency and defect localization. Eddy current testing [6–8] is just an inspection method applied to conductive materials. The information of the bond coat thickness changing and pores size varying can be reflected through measuring the coil impedance. This technology has a high sensitivity but it can’t detect the exact location and shape of the cracks. Similarly, impedance spectroscopy detection method [9,10] measures the changing coating electrical impedance caused by the variation of oxide layer thickness and coating microstructure. Acoustic emission method [2,11] analyses the acoustic emission signals

✉ Zhanwei Liu
liuzw@bit.edu.cn

✉ Huimin Xie
xiehm@mail.tsinghua.edu.cn

¹ School of Aerospace Engineering, Beijing Institute of Technology, Beijing 100081, China

² AML, Department of Engineering Mechanics, Tsinghua University, Beijing 100084, China

produced by extension of cracks. In response to this situation, infrared thermal wave nondestructive testing technology (IR TWNDT) attracted the interest of many researchers in recent years, because of its numerous advantages like large detection area, fast detection speed, visual results images, non-contact, and no damage. And some nice works have been done on the application of IR TWNDTF to NDT of TBCs [12–15]. The position and depth of the defects in TBCs can be obtained in lamp thermography [16]. Quantitative measurement of the coating thickness during production has been achieved in pulsed thermography [17]. The translucency of ceramic layer in transient thermography was analyzed and this affect can be eliminated by using a long-wavelength IR camera [18,19]. Quality evaluation for TBCs has been studied by analyzing thermal stability and mechanical properties [17,20,21]. Some additional effects on the heat conduction related to the crack detection were analyzed and thought, such as multiple reflections of the heating light beam inside the sample, heat losses by convection and radiation [19,22]. But for surface cracks by using IR TWNDT, the typical multi-layer materials, the thin thickness, porous and low thermal conductivity of ceramic coat in TBCs, the interference of the bond coat and substrate, may be the limiting factors of IR TWNDT applied to the surface cracks detection. And related works are mainly focused on some simple structures like steel plate which has single material and high thermal conductivity [22–25]. A ‘flying spot camera’ system heating a sample with a moving laser spot and observing the temperature change with an IR detector was developed to detect crack in metal materials [26,27]. Similarly, a ‘line scan camera’ system was used to inspect the defects in large aircraft fuselage [28,29].

With laser scanning system and IR camera, a new thermal excitation method called the laser multi-mode scanning thermography method is proposed in this paper to detect the surface crack in TBCs. Compared with most of the surface heating used in the existing methods, the thermal response features stimulated by the linear laser are clearer and more intuitive. The scanning process is divided into two stages: line-scan stage (rough scanning) and point-scan stage (fine scanning). In the first stage, a linear laser scanning on the specimen surface, the thermal images collected by IR camera will present unique thermal response features when the laser scanned crack defects, and subsequent thermal images analysis based on these features can obviously reveal the shape and position of the defects. In the process of Line-scan stage, there may be some fuzzy areas where it is difficult to determine whether there is a crack or not, and this is often caused by the too narrow crack width and low resolution of IR camera. For these suspected crack areas, the Point-scan stage can be implemented to detect the narrower crack defects. Line-scan stage, with a rapid scanning speed can quickly detect the wide crack defects in large area range. Point-scan stage,

with high sensitivity, has a better resolution of narrow crack defects. Combination of two scanning modes can alleviate the contradiction of defect detection time and the detection sensitivity, making the defect detection more efficient. Validation tests on real TBCs cracks showed that the SMLT method developed in this paper can efficiently detect the surface cracks with a width of 9.5 μm or more.

2 Principle of Laser Multi-mode Scanning Thermography Method

In order to achieve rapid and accurate detection of micro-cracks of TBC surface, detection process of using the developed laser multi-mode scanning thermography (LMST) method is divided into two stages: line-scan stage and point-scan stage. Their respective principles are introduced here.

2.1 Detection Principle in Line-Scan Stage

2.1.1 Theoretical Analysis

The heat conduction process when line laser scanning specimen surface should be firstly understood to better investigate the thermal response features of defect region. When excitation source of linear laser is applied, a thin layer of material on the specimen surface is instantly heated to a high temperature. Then heat conduction occurs from the surface to the interior of the specimen, resulting in a continuous decline of the surface temperature. Ignoring the air convection heat transfer between the surface and the ambient air and the diffusion heat in the horizontal direction, heat conduction process can be simplified as a one-dimensional heat conduction along the thickness direction in adiabatic boundary [30]. The decrease of the surface temperature T with time t is expressed as follows [31]:

$$T(t) = \frac{Q}{\rho CL} \left[1 + 2 \sum_{n=1}^{\infty} \exp\left(-\frac{n^2\pi^2}{L^2}\alpha t\right) \right] \quad (1)$$

where Q is the total heat energy deposited on the specimen surface, ρ is the material density, C is the specific heat, L is the specimen thickness, α is the thermal diffusivity, and t is the time. Equation (1) shows that surface temperature of the specimen is closely related to the thermal diffusivity.

However, the existence of surface crack that is filled with air changes the local morphology and thermal parameters of TBCs surface. The thermal conductivity of ceramic (normal region) and air (defect region) is respective $1.5 \text{ (W} * (\text{m} * ^\circ\text{C})^{-1})$ and $0.07 \text{ (W} * (\text{m} * ^\circ\text{C})^{-1})$, which means that the heat transfer will be obstructed and the temperature at the defect will be higher.

Table 1 The thermal and physical properties of TBC model

Structure and material	$\rho/(\text{kg}\cdot\text{m}^{-3})$	$C/(\text{J}\cdot(\text{kg}\cdot^\circ\text{C})^{-1})$	$\lambda/(\text{W}\cdot(\text{m}\cdot^\circ\text{C})^{-1})$
Substrate (GH4037)	8400	377	10.9
Ceramic coat (TGR-03, $\text{ZrO}_2 + 8\%\text{Y}_2\text{O}_3$)	5400	600	1.5
Air	1.2	1005	0.07

When the line laser is scanning on the specimen surface with crack defects, the surface temperature distribution (T) at each position (x, y) is divided into four parts: the temperature of the unheated intact region T_{0-back} ; the temperature of the heated intact region T_{0-heat} ; the temperature of the unheated cracks region $T_{crack-back}$; the temperature of the heated cracks region $T_{crack-heat}$. The specific expression is as follows:

$$T(x, y, t) = \{T_{0-back}(t), T_{0-heat}(t), T_{crack-back}(t), T_{crack-heat}(t)\} \quad (2)$$

From the Eq. (2), it could be expected that if using a linear laser instead of planar laser to scan a TBC specimen surface with a crack, abundant distinct features related to temperature variation may be emerged in temperature fields. These features of temperature variation include both in spatial domain and temporal domain variations. Compared with other thermal excitation modes, some of these features may be unique one, which could be applied to fast NDT for surface cracks in TBCs.

According to the above basis, the corresponding simulation by ABAQUS is also carried out, and the characteristics of thermal response of a crack by using linear laser scanning and heating are analyzed and summarized.

2.1.2 Finite Element Simulation and Features Analysis

The used physical parameters of the TBCs model are from the document, which is shown in Table 1. The size of the simulated TBC specimens is $20 \times 20 \times 2 \text{ mm}^3$, the thickness of the ceramic layer is $400 \mu\text{m}$, and a crack near the center of specimen surface has $100 \mu\text{m}$ width and $200 \mu\text{m}$ depth.

It is important to note that a real specimen with a crack of unknown location and direction, will show different temperature responses when the direction of linear laser scanning is parallel, perpendicular or intersecting with the crack. In order to simulate real detection procedure, the linear heat source scanned across the crack in different directions: vertical scanning (Fig. 1a), inclined scanning (Fig. 1b) and parallel scanning (Fig. 1c).

In the process of vertical scanning, the direction of linear laser scanning and heating is perpendicular to that of crack length (Fig. 2a). Since the radiation coefficient at the crack is higher than other positions, meanwhile, the crack surface

area available to adsorb heat is also larger than other normal region, thus the temperature at the intersection position of linear heating source and crack has a significant rise (Feature 1, Fig. 2b). The heat dissipation rate at crack is slower than other positions, which makes the temperature image change near the crack, generating high residual temperature after linear laser scans the crack. Fig. 2c shows that a linear temperature image is dragged, and a ‘tailing’ phenomenon (Feature 2) behind the linear laser obviously appears for a relatively long moment along with the linear laser scanning going through the whole crack defect.

In the process of inclined scanning, the linear laser is scanning at a certain inclined angle with the crack (Fig. 3a). It’s worth noting that, apart from a higher temperature region at intersecting location between linear laser and the crack (Fig. 3b and c), another obvious phenomenon, ‘dislocation’ in temperature images (Feature 3) near the crack, often occurs for inclined scanning (Fig. 3b). This is because the upper end surface and lower end surface of the crack is disconnected and discontinuous, in which thermal conductivity is blocked and drastic changes. When scanning on the crack, the linear laser is heating on different stagger position of upper end surface and lower end surface, respectively. These reasons above cause the ‘dislocation’ phenomenon in the temperature image. In addition, a ‘tailing’ dragged behind the linear laser during inclined scanning is also distinct (Fig. 3c).

In the process of parallel scanning (Fig. 4b), when the linear laser has scanned the crack, the temperature at the overlapping region elevates to the highest. And the area of with high temperature increase to the peak (Feature 4) after the linear laser just scans through the crack (Fig. 4c) and the dragged phenomenon also occurs.

In Line-scan stage, vague shape and low contrast in temperature images with slightly high temperature may appear usually due to the narrow width of tested crack and low resolution of IR camera. For these suspected defect regions, Point-scan method is developed to further ascertain them.

2.2 Detection Principle in Point-scan Stage

Since the thickness of TBC structure is much smaller than its length and width, if ignoring the thermal conduction in thickness direction, a point heating process can be described by the law of two-dimensional Fourier heat conduction:

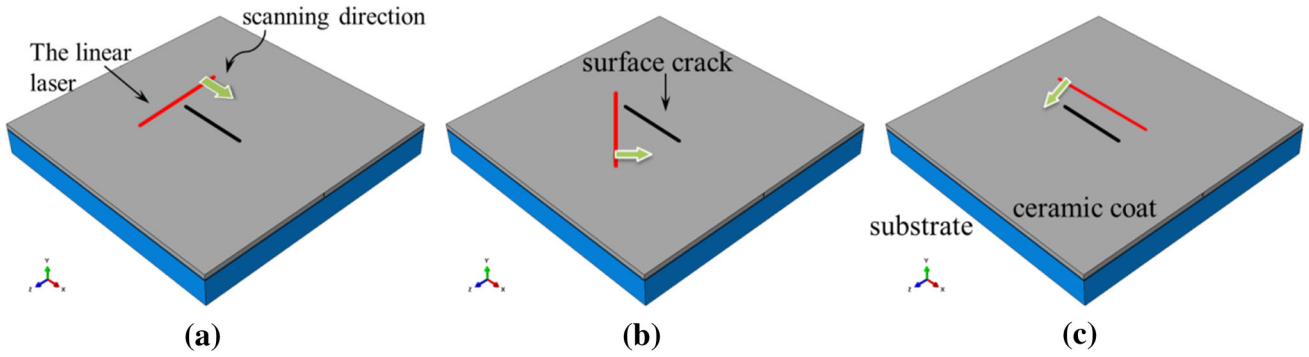


Fig. 1 Multi-angle scanning through the crack with linear laser. **a** Vertical scanning, **b** inclined scanning, **c** parallel scanning

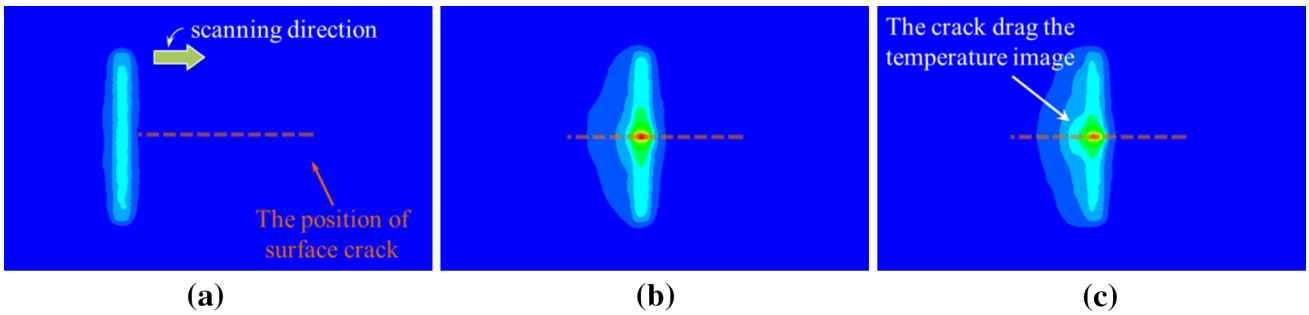


Fig. 2 Variation of temperature field during linear laser vertical scanning. **a** Before scanning, **b** During scanning, **c** A 'tailing' dragged behind the linear laser after scanning

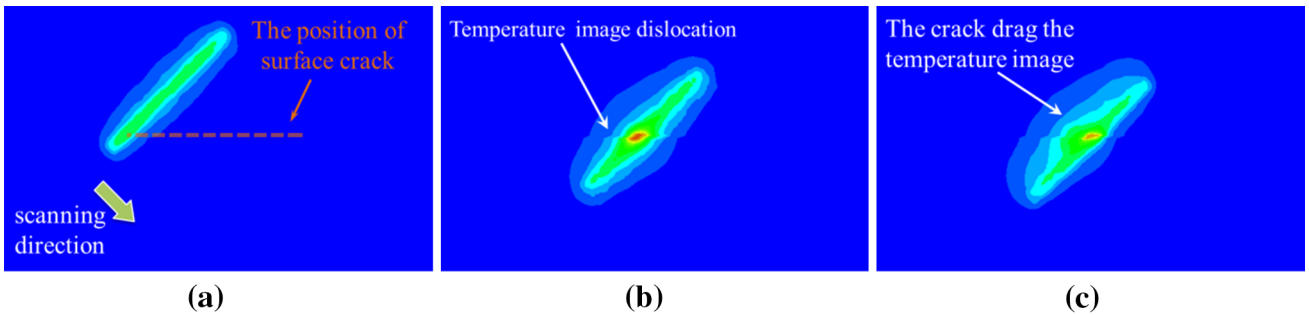


Fig. 3 Temperature field variation during linear laser inclined scanning. **a** Before scanning, **b** A 'dislocation' and higher temperature region at intersecting location during scanning, **c** A 'tailing' dragged behind the linear laser after scanning

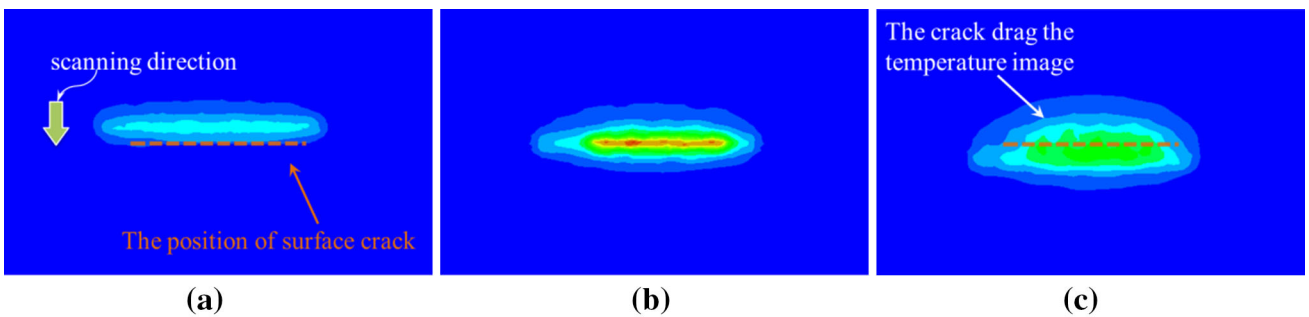


Fig. 4 Temperature field variation during linear laser parallel scanning. **a** Before scanning, **b** The temperature at the overlapping region is the highest during scanning, **c** After scanning

$$\begin{aligned}
 & q_x(x, y) \cdot \vec{i} + q_y(x, y) \cdot \vec{j} \\
 & = -\lambda(x, y) \cdot \left(\frac{dT(x, y)}{dx} \cdot \vec{i} + \frac{dT(x, y)}{dy} \cdot \vec{j} \right) \quad (3)
 \end{aligned}$$

where, T is the temperature on specimen surface, \vec{q} is heat flux density, and λ is the thermal conductivity of material.

During the scanning process of a point heating source, the absolute value of temperature gradient can be expressed as:

$$\begin{aligned}
 & \left| \frac{dT(x, y)}{dx} \cdot \vec{i} + \frac{dT(x, y)}{dy} \cdot \vec{j} \right| \\
 & = \frac{\left| q_x(x, y) \cdot \vec{i} + q_y(x, y) \cdot \vec{j} \right|}{\lambda(x, y)} \\
 & = Q \cdot \left[\frac{1}{r_0 \cdot \lambda_0}, \frac{1}{r_{crack} \cdot \lambda_{crack}} \right] \quad (4)
 \end{aligned}$$

where, Q is the heat flux parameter, associated with the power of the point heat source, r is the distance from a tested point to the center of the point heating source. For TBC surface with surface cracks, the distribution of thermal conductivity λ can be divided into two parts: surface crack region λ_{crack} ($\lambda_{crack} \approx \lambda_{air}$) and intact region λ_0 ($\lambda_0 = \lambda_{ceramic}$). Here, the thermal conductivity of air $\lambda_{air} = 0.07$, the thermal conductivity of ceramic $\lambda_{ceramic} = 1.5$.

Equation 4 shows that, the temperature gradient is affected by the distance from the crack to the heating point and the thermal conductivity ratio $\lambda_{crack}/\lambda_0$. A point heating process with different distance from the crack is simulated and shown in Fig. 5. From the simulation result, when the point heat source is close to the crack, the thermal obstruction phenomenon (Feature 5) becomes more obvious in Fig. 5c and d. It's noted that, although the thermal obstruction phenomenon is more obvious when the point heat source is closer to the crack, if the distance is too close, effective thermal diffusion will be missing, and the crack length detected by using temperature gradient is smaller than that when there is a suitable distance between crack and the point heat source.

From above analysis, all the distinct features are summarized as follows:

- (1) *Distinct Features 1* local position points with abnormal temperature
Some certain location points with special higher temperature variation will be identified in temperature distribution images where the scanning linear laser intersects the crack. These location points are exactly a part of the crack waited for NDT. Thus, the shape and location of the whole surface crack will be reconstructed by capturing and connecting all such location points.
- (2) *Distinct Features 2* unique 'tailing' phenomenon
On account of slow heat dissipation at cracks position, after the linear laser continuously scans through a crack,

the temperature distribution will be dragged near the crack region, forming a wake like the tail of a comet. This unique 'tailing' is one of the important features, which doesn't exist in other thermal stimulation, such as plane light source.

- (3) *Distinct Features 3* unique 'dislocation' phenomenon
A 'dislocation' phenomenon in temperature images is distinctly emerged near cracks only during inclined scanning. Compared with most of the surface source used in the existing methods, it is also a new and unique feature.
- (4) *Distinct Features 4* distinct increase of the area of high temperature zone
The shape of the surface cracks is generally similar to a straight line or an arc. In the condition that the scanning linear heat source is parallel to the crack or the angle between them is small, there will be a large overlapping high temperature zone when linear heat overlaps the crack. For the temperature image of each frame in the scanning process that linear laser close to the crack, overlapping and finally over the crack, the area of high temperature will show a trend that increases first and then decreases, peaked when overlapping. In other words, under the circumstances that the angle between linear laser and crack is smaller, the area of high temperature will reach a peak in the crack location.
- (5) *Distinct Features 5* obvious thermal obstruction phenomenon
The low thermal conductivity hinders heat conduction through the cracks when using a point heat source scanning, which results in the temperature gradient sharply varied at cracks.

The five above thermal response features aroused by linear laser and point laser scanning can be conveniently and visually applied to NDT for cracks.

3 Validation Tests and Result Discussion

3.1 Specimens and LMST System

A LMST system is established with a semiconductor laser marking machine and an IR camera. The schematic diagram of the experimental apparatus is shown in Fig. 6. The semiconductor laser marking machine can converge a laser spot (minimum diameter of 0.05 mm), and the laser point is controlled to move quickly in a straight direction. The laser point can be viewed as a linear laser when the scanning speed is sufficiently fast and a linear movement is made. This laser point can be considered a linear excitation when the linear laser scanning direction is perpendicular to the moving direction, as shown in Fig. 6a. By adjusting the moving path of

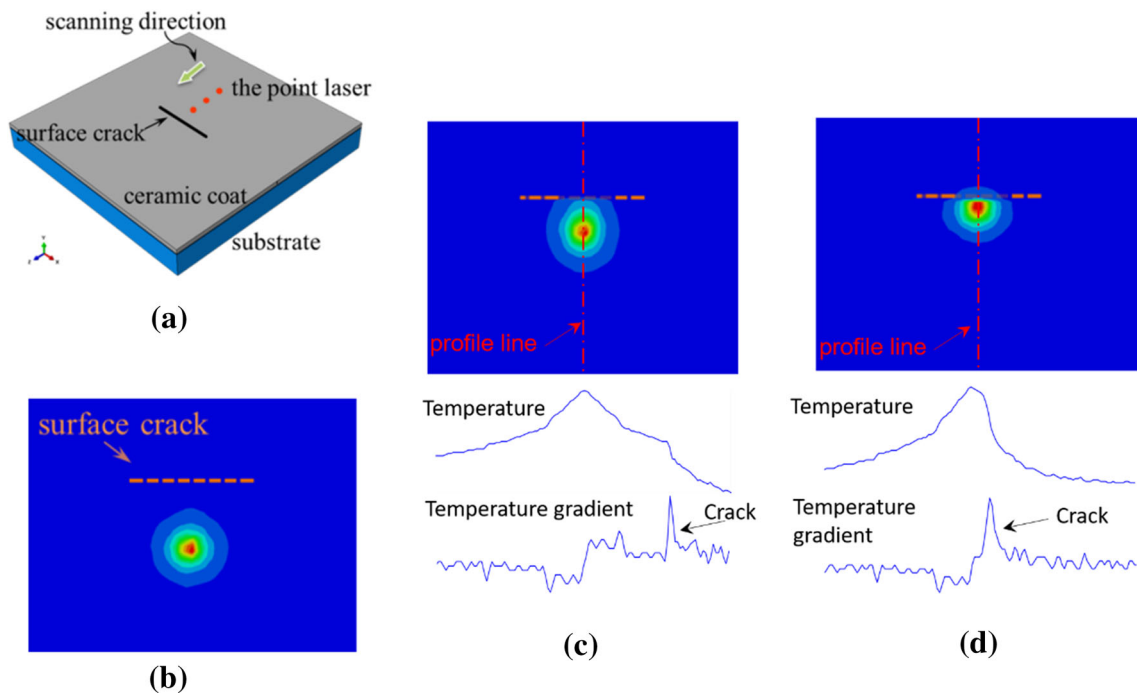


Fig. 5 The simulation of fine scanning. **a** Scanning schematic of point heat source in fine scan stage. **b** The temperature image when point heat source is far away from the crack. **c** The temperature image when point heat source approaches to the crack (above), temperature profile

(middle) and temperature gradient (below). **d** The temperature image when point heat source is very close to the crack (above), temperature profile (middle) and temperature gradient (below)

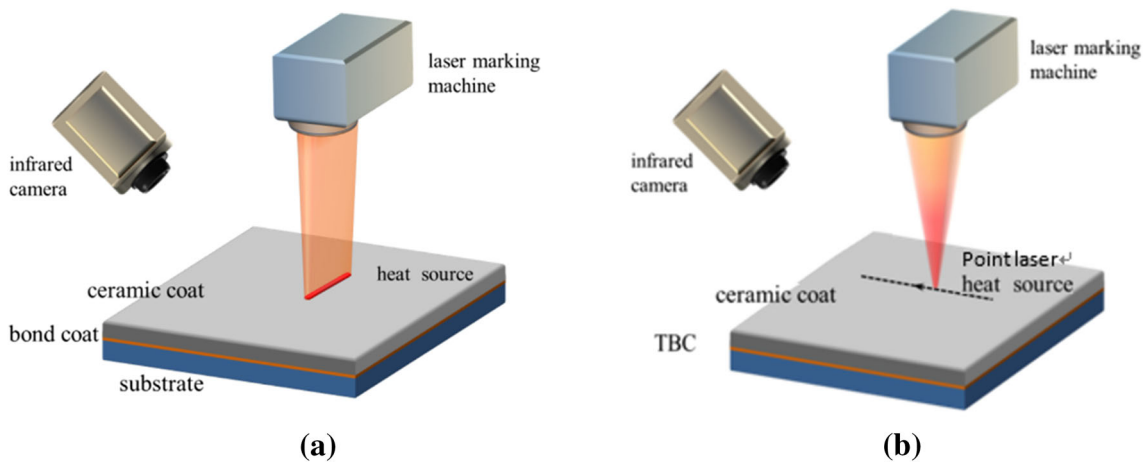


Fig. 6 Schematic diagram of the experimental apparatus

the laser spot, the switching between point scanning (Fig. 6b) and linear scanning mode can be realized.

The TBC specimens used here are conventional plasma-spray deposited coating structure, which consists of substrate of nickel base alloy, bond coat and ZrO_2 ceramic coat, and their thickness are 2000, 100 and 400 μm , respectively. Surface cracks were fabricated on TBC specimen surface by mechanical stretching method using TBC tensile specimens. For the specimen (shown in Fig. 7), there are three main cracks whose width are from 19 to 98 μm .

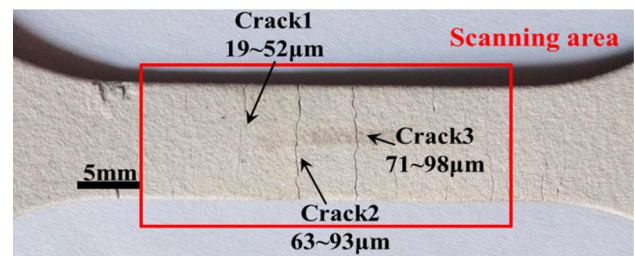


Fig. 7 TBC specimen with three main cracks

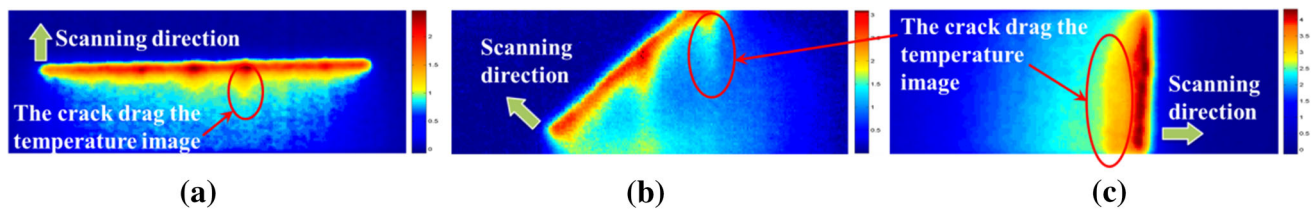


Fig. 8 Thermal response features during linear laser scanning. **a** Vertical scanning. **b** Inclined scanning. **c** Parallel scanning

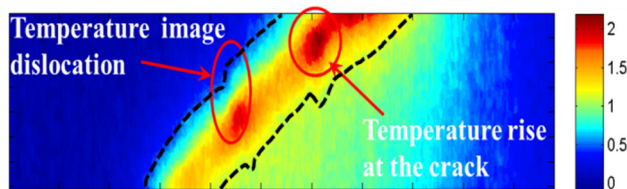


Fig. 9 'Dislocation' phenomenon in temperature image by slowly scanning

3.2 Linear Laser Scanning Test

In order to exhibit evident thermal response features of cracks, some laser parameters such as moving speed and the size of laser point, and scanning speed of linear laser, need to be optimized firstly. If scanning speed is too fast, there will be not enough heating time, causing the thermal response at the crack too weak to be distinguished. However, if too slow will cause overheating at surface cracks, and the temperature distribution near cracks tends to be uniform. Both of these two cases reduce the thermal images contrast between cracks and other normal region, thus obstruct the final crack detection. The optimized scanning speed of the linear laser is controlled from 1 to 10 mm/s, the laser point diameter is from 0.1 to 0.3 mm with a moving speed of 500 mm/s.

When a linear laser is scanning across the specimen surface with three cracks (Fig. 7) along different directions, some significant thermal response features were observed. The experimental result is shown in Fig. 8. In vertical scanning (Fig. 8a), three unusual positions with highest temperature value indicate the position of the cracks (Feature 1). 'Tailing' phenomenon (Feature 2) is also very distinct not only in vertical scanning and inclined scanning (Fig. 8b), but in parallel scanning (Fig. 8c). In parallel scanning, distinct increase of the area of high temperature zone (Feature 4) is clearly observed.

In addition, the unique 'dislocation' phenomenon (Feature 3) also can be observed when the scanning speed is slow down to 1 mm/s, as shown in Fig. 9.

The above phenomenon reflects the information of cracks, in which the temperature increasing at cracks is the most common. When processing the temperature images captured by IR camera using the binarization method, the binarization threshold is a critical factor. Appropriate threshold can

effectively shield the noise, and highlight the position of the cracks. There are two methods for determining the threshold value: one is to average the temperature of the region irradiated by the line laser during the scanning process. Because the cracks and other defects account for a small portion of overall specimen, the average temperature T_0 can be considered as a carrier temperature when the linear laser irradiates on the specimen surface with no defect. Choose a temperature T_1 which is slightly larger than T_0 as the threshold value of every frame temperature image during the scanning. The advantage of this method is that the reconstructed results wouldn't be affected by the temperature changing caused by other defects such as surface impurity. The other method for determining the threshold value is to choose the 90% of highest temperature in each image with thermal response features as the threshold value. And then, each temperature image has its own threshold. The advantage is that the influence of heat accumulation during scanning processing is reduced. In experiment, we perform weighted average of the two threshold values processing results to obtain the final result. Taking the vertical scanning as an example, the cracks reconstruction process and the final result are shown in Fig. 10a–d.

From the Fig. 10, it can be seen that vertical scanning can fast identify crack2 and crack3, whose width is larger than 20 μm . As for crack1, the thermal response features are not clear, so it can be considered as a suspected crack, and the further confirmation need to be conducted by the fine scanning using point laser scanning.

3.3 Point-scan for Detecting Micro Cracks

The suspected crack in the specimen of Fig. 10d was detected using a point laser scanning. When a point laser moves toward the micro-crack in a certain direction, the heat conduction will be impeded by the crack (upper image in Fig. 11a), and the temperature gradient value near crack will have a significant abnormality (lower image in Fig. 11a). Figure 11b is the full field temperature gradient image, and after thinning the binaryzation result of the temperature gradient (Fig. 11c), shape and location the suspected crack can be visually presented. By accumulating all of such thinning result of temperature gradient binaryzation for all temperature images in time series and combining with the results of linear laser

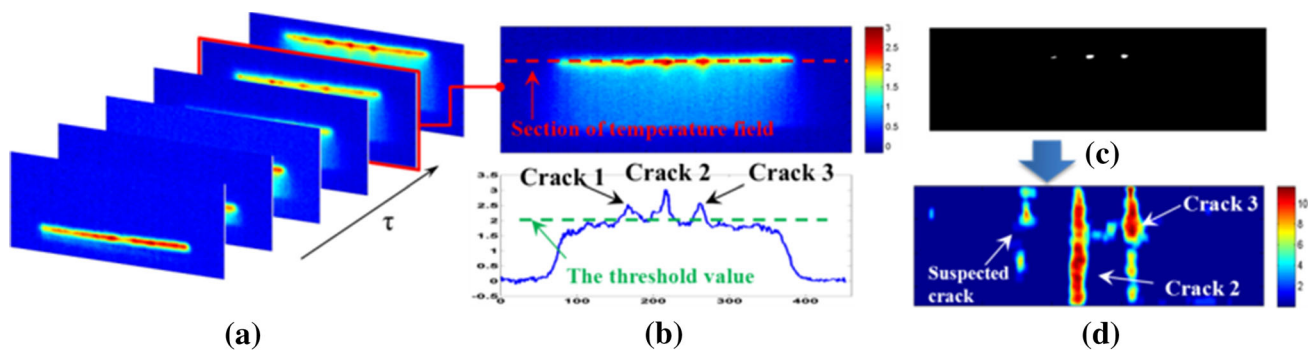


Fig. 10 The reconstruction process of three cracks in vertical scanning. **a** The original temperature images in time series. **b** The temperature image at a certain moment and its temperature distribution in one section. **c** The threshold extraction result at this moment. **d** The reconstruction result

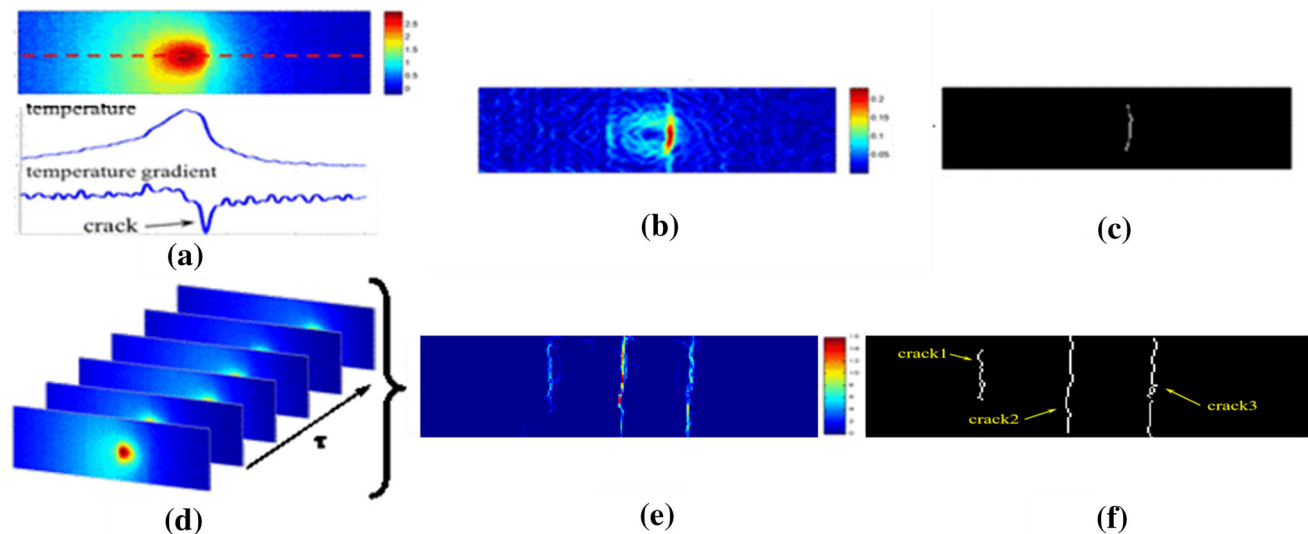


Fig. 11 The process of the point laser scanning stage. **a** Temperature image at a moment (above), temperature section (middle) and temperature gradient (below). **b** Gradient distribution of temperature field at a moment. **c** Thinning the binaryzation result of the temperature gradient

at a moment. **d** The original temperature images in time series. **e** The accumulation result of temperature gradient at each moment. **f** The final result by combining rough scanning with fine scanning

scanning, all cracks can be displayed in the scanning range, as shown in Fig. 11d–f.

3.4 The Detection Sensitivity for Micro-Cracks

To better understand the detection sensitivity for micro-cracks, some narrower surface cracks were fabricated by using stretching fatigue method (shown in Fig. 12). The average width of the cracks is 11.2 μm, the average spacing of between cracks is 0.93 mm. The cracks are too narrow to be observed, so a mark line is drew to make the positions easy to be located. Thus, the actual positions of the cracks in the temperature image are determined by using the mark line and then the cracks width will be measured by a microscope, and the detection sensitivity of the method can be confirmed.

For the narrower surface cracks, the scanning speed should slowly down to provide enough time for thermal diffusion.

The laser spot need to be as small as possible to increase the measurement accuracy, the selected spot diameter is 0.1 mm in this investigation. During scanning, the temperature increases quickly in the heating micro-region due to small diameter of the laser point, and the temperature gradient in this region is very large, which shields the gradient information of cracks beyond the spot laser. In order to reduce this influence, the temperature values in the position of laser point are assigned to be empty. By this way, the temperature gradient information around the laser spot can be highlighted, as shown in Fig. 13b.

Figure 13 shows that there are different temperature gradient results in the heating process where heating for two seconds and then the point laser is removed. During the heating phase (Fig. 13, time 1), the temperature gradient in the heating region is too large and shields the gradient information of other region. In the early period of heat dissipation

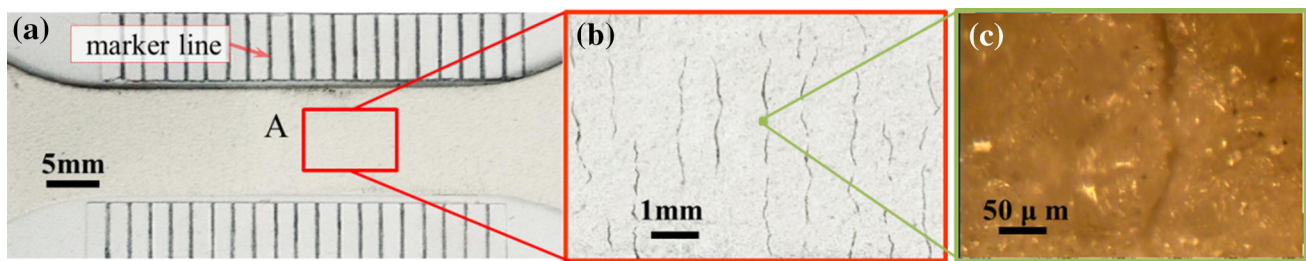


Fig. 12 TBC tensile specimen II. **a** Specimen II with mark line. **b** Microscopic image of point A. **c** Zoom in of the b

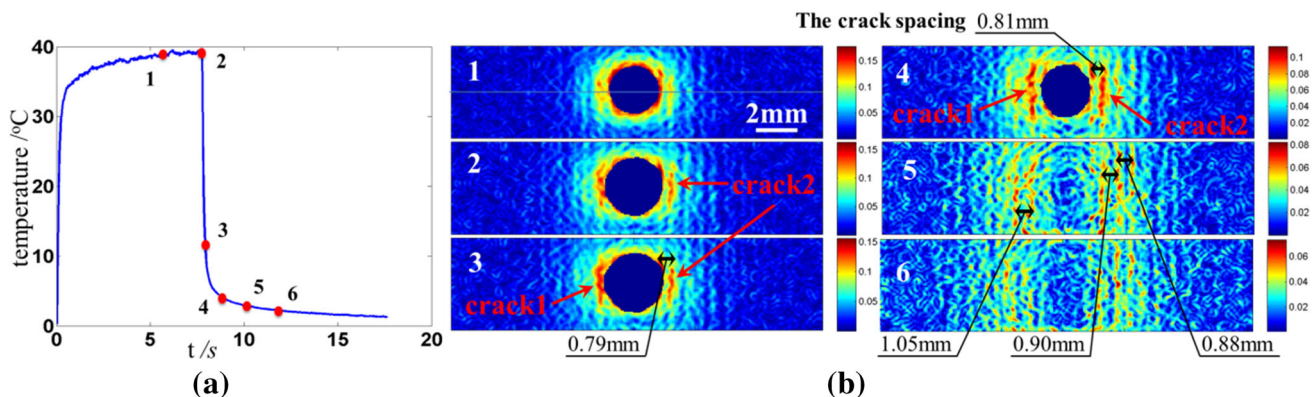


Fig. 13 The temperature distribution of point A and temperature gradient images at all times. **a** Temperature–time curve at point A. **b** The temperature gradient results of the whole image at time 1–6

(Fig. 13, time 3, 4), the gradient information of the cracks is the most significant. In the end period of heat dissipation (Fig. 13, time 6), the low contrast of temperature-gradient hinders the crack identification. Taking full advantage of the processed results in early period of heat dissipation, these cracks can be detected accurately. The detected width of crack1 and crack2 is 11.2 and 9.5 μm , respectively (validated by an optical microscope). This indicates that in point-scan stage, micro-cracks with width of 9.5 μm can be detectable. Besides, the average pitch of these cracks also can be detected from the gradient image, which is 0.89 mm, similar to the observation result using optical microscope.

4 Conclusion

Aiming at NDT for the surface cracks in TBCs, a laser multi-mode scanning thermography (SMLT) method has been developed in this paper. Two scanning modes, linear-scanning and point-scanning, are combined to scan quickly on the surface of the specimen by using the built scanning system. Through numerical simulation and experimental verification, four thermal response features in Line-scan stage and one thermal response feature in Point-scan stage are utilized to highlight the shape and position of defects. Compared with most of the surface scanning used in the existing methods, the two features which are ‘tailing’ phenomenon

and ‘dislocation’ phenomenon are new and unique. Among them, the ‘tailing’ phenomenon emerging after linear laser scanning is the most practical, because the thermal response features of the defect are more obvious during the heating phase than in the cooling phase. In the real experiment, large defects with the width of 20 μm or more can be detected with fast speeds and large detection range in the rough stage, and the suspected defects found in the rough stage can be detected with higher sensitivity and smaller detection range in the fine stage. It is shown that combining the two scanning modes with the developed post-processing algorithm, the surface crack with the width of more than 9.5 μm in TBCs can be accurately detected with high efficiency.

Acknowledgements This work was financially supported by the National Natural Science Foundation of China [Grant No. 11372037, 11572041, and 11232008].

References

- Zhu, D. M., Miller, R. A.: Thermal and environmental barrier coatings for advanced propulsion engine systems. In: NASA Technical Memorandum 1 (2004)
- Yang, L., Zhou, Y.C., Lu, C.: Damage evolution and rupture time prediction in thermal barrier coatings subjected to cyclic heating and cooling: an acoustic emission method. *Acta Mater.* **59**(17), 6519–6529 (2011)

3. Yang, L., Zhou, Y.C., Mao, W.G., Liu, Q.X.: Acoustic emission evaluation of the fracture behavior of APS-TBCs subjected to bondcoating oxidation. *Surf. Interface Anal.* **39**(9), 761–769 (2010)
4. Ghasemi, R., Shoja-Razavi, R., Mozafarinia, R., Jamali, H.: The influence of laser treatment on thermal shock resistance of plasma-sprayed nanostructured yttria stabilized zirconia thermal barrier coatings. *Ceram. Int.* **40**(1), 347–355 (2014)
5. Zhou, B., Kokini, K.: Effect of surface pre-crack morphology on the fracture of thermal barrier coatings under thermal shock. *Acta Mater.* **52**(14), 4189–4197 (2004)
6. Yong, L., Chen, Z., Mao, Y., Yong, Q.: Quantitative evaluation of thermal barrier coating based on eddy current technique. *Ndt E Int.* **50**, 29–35 (2012)
7. Khan, A.N., Khan, S.H., Ali, F., Iqbal, M.A.: Evaluation of ZrO-24MgO ceramic coating by eddy current method. *Comput. Mater. Sci.* **44**(3), 1007–1012 (2009)
8. Biju, N., Ganesan, N., Krishnamurthy, C.V., Balasubramaniam, K.: Defect sizing simulation studies for the tone-burst Eddy current thermography using genetic algorithm based inversion. *J. Nondestruct. Eval.* **31**(4), 342–348 (2012)
9. Huang, H., Liu, C., Ni, L., Zhou, C.: Evaluation of TGO growth in thermal barrier coatings using impedance spectroscopy. *Rare Met.* **30**(1), 643–646 (2011)
10. Huang, H., Liu, C., Ni, L., Zhou, C.: Evaluation of microstructural evolution of thermal barrier coatings exposed to Na₂SO₄ using impedance spectroscopy. *Corros. Sci.* **53**(4), 1369–1374 (2011)
11. Mohan, R., Prathap, G.: An acoustic emission energy analysis and its use to study damage in laminated composites. *J. Nondestruct. Eval.* **1**(4), 225–233 (1980)
12. Franke, B., Sohn, Y.H., Chen, X., Price, J.R., Mutasim, Z.: Monitoring damage evolution in thermal barrier coatings with thermal wave imaging. *Surf. Coat. Technol.* **200**(5–6), 1292–1297 (2005)
13. Marinetti, S., Robba, D., Cernuschi, F., Bison, P.G., Grinzato, E.: Thermographic inspection of TBC coated gas turbine blades: discrimination between coating over-thicknesses and adhesion defects. *Infrared Phys. Technol.* **49**(3), 281–285 (2007)
14. Ghiassi, B., Silva, S.M., Oliveira, D.V., Lourenço, P.B., Bragança, L.: FRP-to-masonry bond durability assessment with infrared thermography method. *J. Nondestruct. Eval.* **33**(3), 427–437 (2014)
15. Ptaszek, G., Cawley, P., Almond, D., Pickering, S.: Artificial disbands for calibration of transient thermography inspection of thermal barrier coating systems. *NDT E Int.* **45**(1), 491–498 (2012)
16. Sun, J.G.: Analysis of pulsed thermography method for defect depth prediction. *J. Heat Trans.* **128**(4), 329–338 (2006)
17. Zhao, S.B., Zhang, C.L., Nai-Ming, W.U., Wang, H.M.: Quality evaluation for air plasma spray thermal barrier coatings with pulsed thermography. *Prog. Nat. Sci.* **21**(04), 301–306 (2011)
18. Ptaszek, G., Cawley, P., Almond, D., Pickering, S.: Transient thermography testing of unpainted thermal barrier coating (TBC) systems. *Ndt E Int.* **59**(1), 48–56 (2013)
19. Salazar, A., Mendioroz, A., Apiñaniz, E., Pradere, C., Noël, F., Batsale, J.C.: Extending the flash method to measure the thermal diffusivity of semitransparent solids. *Meas. Sci. Technol.* **25**(3), 035604 (2014)
20. Cernuschi, F., Capelli, S., Bison, P.: Non-destructive thermographic monitoring of crack evolution of thermal barrier coating coupons during cyclic oxidation aging. *Acta Mater.* **59**(16), 6351–6361 (2011)
21. Bison, P.G., Federico Cernuschi, Ermanno Grinzato: Ageing evaluation of thermal barrier coating: comparison between pulsed thermography and thermal wave interferometry. *Quant. Infrared Thermogr. J.* **3**(2), 169–181 (2006)
22. Celorrio, R., Omella, A.J., Pechmay, N.W., Oleaga, A., Mendioroz, A., Salazar, A.: Vertical cracks characterization using lock-in thermography: II finite cracks. *Meas. Sci. Technol.* **25**(11), 115601 (2014)
23. Burrows, S.E., Dixon, S., Pickering, S.G., Li, T., Almond, D.P.: Thermographic detection of surface breaking defects using a scanning laser source. *NDT E Int.* **44**(7), 589–596 (2011)
24. Li, T., Almond, D.P., Rees, D.A.S.: Crack imaging by scanning pulsed laser spot thermography. *NDT E Int.* **44**(2), 216–225 (2010)
25. An, Y.K., Ji, M.K., Sohn, H.: Laser lock-in thermography for detection of surface-breaking fatigue cracks on uncoated steel structures. *NDT E Int.* **65**(5), 54–63 (2014)
26. Krapez, J.C.: Spatial resolution of the flying spot camera with respect to cracks and optical variations. In: *Proceedings of the International Conference on AIP*, pp. 377–379 (1999)
27. Gruss, C., Lepoutre, F., Balageas, D.: Nondestructive evaluation using a flying-spot camera. In: *Proceedings of the International Conference on Thermo*, (1993)
28. Woolard, D.F., Cramer, K.E.: Line scan versus flash thermography: comparative study on reinforced carbon-carbon. In: *Proceedings of The International Society for Optical Engineering*, SPIE-5782 (2005)
29. Woolard, D.F., Cramer, K.E.: The thermal photocopy: a new concept for thermal NDT. *Proc. SPIE* **5405**, 366–373 (2004)
30. Chang, D.M., Wang, B.L.: Transient thermal fracture and crack growth behavior in brittle media based on non-Fourier heat conduction. *Eng. Fract. Mech.* **94**, 29–36 (2012)
31. Parker, W.J., Jenkins, R.J., Butler, C.P., Abbott, G.L.: Flash method of determining thermal diffusivity, heat capacity, and thermal conductivity. *J. Appl. Phys.* **32**(9), 1679–1684 (1961)